

# Energization of step-up transformers for MV wind-farms: Description of the methodology for the modeling of the equipment and its validation by on-site tests

M. Rioual, J-C. Reveret

**Abstract--**The voltage quality of the energy delivered is a major issue for wind-farms owners and also for the Distribution networks operators. The no load energization of step-up transformers of wind-farms from the Distribution network may lead to high inrush currents and lead to high overvoltages which may affect, in certain cases, the power quality.

The phenomena involved are described in the case of a 2.05 MVA 20kV/960V transformer, with a detailed description of the modeling of the network.

A comparison between simulations and on site tests is firstly presented in the case of the energization of one transformer alone.

**Keywords:** wind-farms, residual flux, transformer, energization, inrush currents, circuit breakers, on site test.

## I. INTRODUCTION

The connection to the Distribution Network in France is submitted to several technical constraints [1]; among them, the voltage dip when coupling such a production system must not exceed 5% at the Connection Point.

This can be caused by the energization of transformers, which may create the saturation of the magnetic core and lead to high overvoltages and inrush currents [2].

The magnitude of those stresses may depend on the following different parameters:

- Closing times of the circuit breakers poles,
- Residual fluxes in the iron core of transformers,
- Transformer parameters as the winding connections, the hysteretic curve of the magnetic core, the power losses and the stray losses in the windings.

In this case, the study has been performed for a 10 MW wind-farm, including four double fed machines having a rated power of 2.5 MVA each.

Firstly, this paper describes the EMTP modeling of the network to be considered, using the EMTP-RV program [5]; in

---

M. Rioual is a IEEE senior member, working at EDF company in the Department of Transformer Group (e-mail of corresponding author: michel.rioual@edf.fr).

J-C. Reveret is a student of "Ecole Speciale de Mécanique et d'Electricité"

Paper submitted to the International Conference on Power Systems Transients (IPST2009) in Kyoto, Japan June 3-6, 2009

particular, the modeling of the 2.05 MVA target transformer is described, with a detailed representation of its saturation characteristics and the underground cable linking the Connection Point to the step-up transformer.

Secondly, a comparison has been made between the simulations performed and the tests made on site, in the case of the energization of one transformer.

## II. METHODOLOGY; DESCRIPTION OF THE MODELING

### A. Description of the Network

The whole meshed network is described in figure 1 below, with the following equipments in the 20 kV Network involved:

- The 15kV/20kV autotransformer for the connection to the Distribution network,
- The MV cable, being 14.7km long and linking the autotransformer to the step-up transformers,
- The 20kV/960V step-up transformers, for the connection to the machines,
- The induction machines.

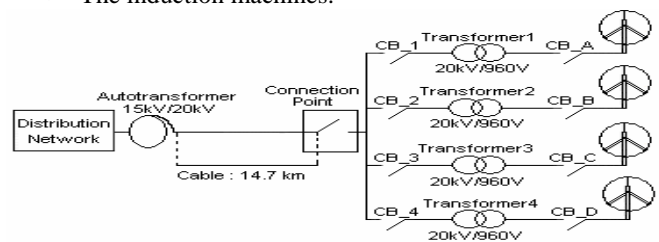


Fig. 1. Description on the Network under study.

In this site, the connections are the following:

- 5 m of cable between the Connection Point and Wind Transformer 1,
- 200 m of cable linking the CP, Wind Transformer 2 and Wind Transformer 4,
- 300m of cable linking the CP and Wind Transformer 3, as described in the figure 2 below:

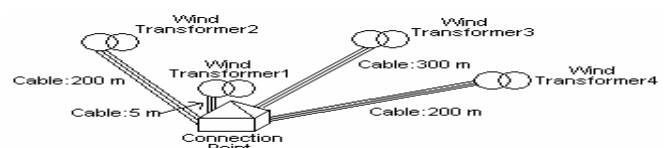


Fig. 2. Description of the C P and the location of the transformers

## B. Modeling of the upstream network and the auto-transformer

### 1) Upstream network

The network equipments have been represented under the phenomena being involved; in particular, the upstream network, as seen from the secondary side of the 15kV/20KV autotransformer, has been represented by a steady-state 20 kV voltage source behind the corresponding short circuit inductance  $L_{sc}$ , and its damping resistance  $R_{sc}$ ; this value is derived from the time constant which characterizes the time for the steady-state short circuit current to occur.

In fact, a more complex modeling has also been used for the modeling of the 15kV/20KV auto-transformer, in order to evaluate its impact on the phenomena involved.

### 2) Autotransformer

In the previous cases performed on this subject [1], the auto-transformer has been represented by an impedance, corresponding to the Joule losses in serie with the magnetic losses; the auto-transformer has also been modeled in a second step by a more complex model, with its saturation curve represented by a non linear inductance as described in fig 3 below:

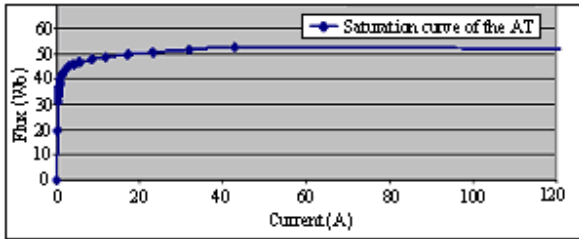


Fig 3. Saturation curve of the auto-transformer on the 15 kV side.

The simulations performed on the energization of one of the step-up transformers of the wind-farm, as described in the following chapters, with both models for the auto-transformer, give the following results:

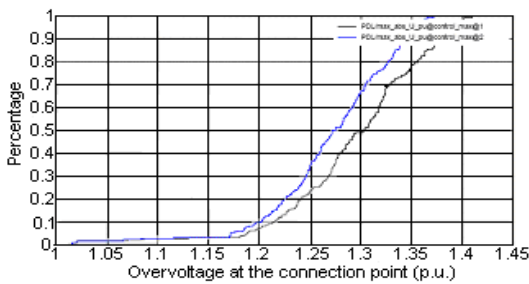


Fig 4. Statistical distribution of overvoltages at the transformer entrance.

As they are very close, with no significant interactions between transformers through the cable, the first modeling has been chosen in the following for the application described in this paper.

The overvoltages are below the withstand level of the equipment, in that case; they may be more critical in the case when the target transformer has a higher rated power, up to 10 MW, the other conditions being the same, especially the short-circuit power of the upstream network.

## C. Modeling of the target transformers

The 2.05 MVA step-up transformers, modeled by three single-phase transformers, are described below, where the leakage inductances, the copper and core losses and the saturation curve are represented:

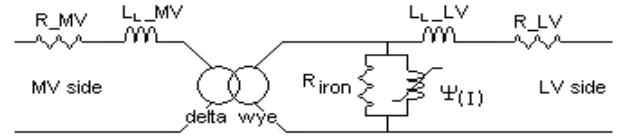


Fig. 5. Description of the step-up transformer modeling (one phase represented).

Those 2.05 MVA transformers, being three limbs transformers, have a delta-wye connection. At the wye connection side, we have represented the saturation inductance by an hysteretic curve [2] and the wye coupling is directly grounded to the earth.

The saturation curve  $\Psi(I)$  is built from the voltage-current curve, where data are given by the manufacturer up to 1.3  $U_n$ . For highly saturation conditions, the parameter  $L_{sat}$  describes the slope, as shown in figure 6 below, and determined with the following formula:

$$L_{sat} = L_{air-core} - L_{leakage}$$

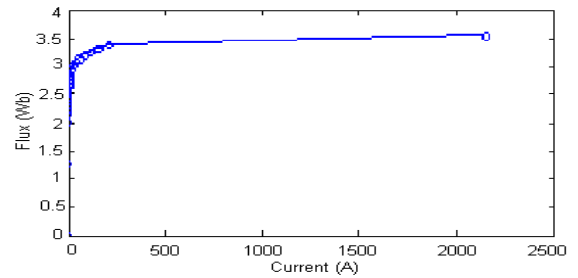


Fig. 6. Saturation curve  $\Psi(I)$  of the 2.05 MVA transformer.

The air-core inductance value  $L_{air-core}$  is given by the manufacturer with an accuracy of 20%; the  $L_{sat}$  parameter, which is the last point on the saturation curve located at the LV side, is fixed at its lowest value 0.12 p.u. (74.6  $\mu$ H) in order to be conservative, where

$$L_{Sat} \text{ (p.u.)} = \frac{\omega * L_{Sat}}{Z_n}$$

The leakage inductance is represented in the modeling and calculated from short circuit tests.

Taking into account the fact that the MV winding is located very close to the iron core, the  $L$  leakage value is divided as follows:

$$90\% \text{ at the MV side: } L_{MV} = \frac{0.9 * U_{cc} * U_{nMV}^2}{\omega * S_n}$$

$$\text{and } 10\% \text{ at the LV side: } L_{LV} = \frac{0.1 * U_{cc} * V_{nLV}^2}{\omega * S_n} .$$

## D. Modeling of the underground cables

### 1) Description of the cable

The cable of the wind-farm site, located in the North of France, is a cable  $3 \times 1 \times 240 \text{ mm}^2$  Copper type C33-226, 14.7 km long.

The cable has the following characteristics, described in figure 7:



Fig. 7. Description of the different layers in the MV cable.

The MV cable is represented by electrical PI cells under the frequencies involved; the number of PI cells has been chosen to eight, in order to represent correctly its exact impedance for the twelfth harmonic which is the resonance frequency of this network.

Each cell is described as shown in figure 8 below:

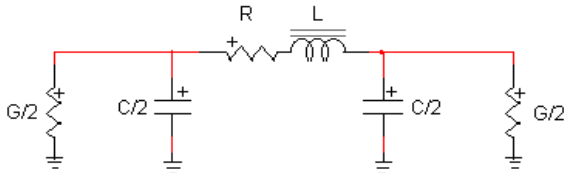


Fig. 8 : A PI-cell for the modeling of the cable (short length) at low frequencies.

It includes the resistance  $R$ , the linear phase to earth capacitance  $C$ , the linear self-inductance  $L$ , the conductance  $G$  and the mutual inductances  $M$  between phases.

The main issue is the determination of those parameters; they can be determined with mathematical formulas for simple cases, but for more complex geometries, the use of tools which generate the elements of the Pi-cell from the electrical and geometrical characteristics may be necessary.

In that case, the ULIS software [6], [7] developed by the R&D Division of EDF for MV cables, which is the reference tool for the ERDF (Distribution network) for the generation of electrical parameters under steady state conditions; it enables the representation of cables where the size of the semi-conductor layers may not be neglected as described below.

In that case, the traditional modeling for EHV cables, which is very powerful for those cables, may not be completely applicable, as the thickness of the semiconductor is not negligible compared to the one of the insulation, which may have an impact on the values of the capacitances [4].

Certain electrical parameters may be estimated in a first step by simple formulas, described below:

### 2) Determination of the conductance $G$ of the cable

It represents the dielectric leakage conduction in the insulation between the two main conductors, the core and the screen; it is mainly characterized by the nature and the state of the insulation, being also dependent on the weather conditions (humidity, temperature, ...). Its value is given by the following expression:

$$G = \frac{2 * \pi * f * C}{Q} * l \quad [1]$$

In the case under consideration, its value is equal to  $9.2 \cdot 10^{-8}$  ohm/km.

### 3) Determination of the resistance $R$ of the cable

It is given by the following formula:

$$R = \rho * (l/S) \quad [2]$$

The software ULIS, which generates a Pi-cell, gives a value very close to the one given by this simple formulae, with a discrepancy within 5%.

### 4) Determination of the linear self-inductance of the cable

The software ULIS provides the self and mutual inductances for the different elements, the screen and the core. It is also possible to determine the linear inductance of cable using the following formulation, which takes into account the distance between the different phases of the cable and the mutual induction between them:

$$L = \frac{\mu_r * \mu_0}{2 * \pi} \left( \frac{1}{4} + \ln \left( \frac{k.D}{R_{\text{conductor}}} \right) \right) * \ell \quad [3]$$

$$\text{N.A: } D = 0.0361 \text{ m; } R_{\text{conductor}} = 0.0091 \text{ m; } k = 1; \mu_r = 1$$

$$\text{N.A: } L = 0.326 \text{ mH/km}$$

$$\text{Data from manufacturer: } L = 0.326 \text{ mH/km}$$

There is a very good match between this formulation and the data provided by the manufacturer, also taken into account in the ULIS software

### 5) Determination of the linear capacity $C$ of the cable

The classic formulation provides for two conductors:

$$C = \frac{2 * \pi * \epsilon_0 * \epsilon_r}{\ln \left( \frac{R_{\text{insulation}}}{R_{\text{conductor}}} \right)} * \ell \quad [4]$$

$$\text{N.A: } R_{\text{insulation}} = 0.0155 \text{ m; } R_{\text{conductor}} = 0.0091; \epsilon_r = 1$$

$$\text{N.A: } C = 260 \text{ nF/km}$$

Note:

The software ULIS gives a value of 367.55 nF/km for the linear capacitance, with a discrepancy of 30% when comparing to the formula described above; in fact, the calculation takes into account the internal and external semiconductors surrounding the conductor and the screen. It gives the following values for the elementary pi-cell:

TABLE I  
ELECTRICAL VALUES OF A PI-CELL FOR THE CABLE DESCRIPTION

Capacity (nF/km)	Inductance (mH/km)	Resistance ( $\Omega$ /km)
367.55	0.326	0.0754

Those values have been used in the following, for the description of one pi-cell.

#### 6) Modeling by several cells Pi

The energization of a transformer generates temporary overvoltages including harmonics, which are injected in the network connected to it; therefore, it is important to have a valid representation of the cable valid for those frequencies, in order to represent its impedance correctly.

In fact, the cable has not been modeled by a frequency dependent modeling, as the ULIS software may provide the pi cells only, with no propagation model yet developed, which is completely suitable under harmonics, when using the right number of pi cells according to the length of the cable and frequencies considered.

We have determined for this cable the influence of the number of pi-cells on its impedance value, considering both the direct sequence and also the zero sequence:

#### Direct sequence :

TABLE II  
INFLUENCE OF THE NUMBER OF PI-CELLS ON THE IMPEDANCE OF THE NETWORK (DIRECT SEQUENCE)

Number of Pi-cells	Impedance ( $\Omega$ )	Resonant frequency (Hz)	Discrepancies (with 8 Pi cells as the reference)
1	6420	598	+ 16 %
2	5735	593	+ 4 %
4	5548	592	+ 0.4 %
8	5524	591	0 %
16	5525	591	+ 0.02 %
50	5528	589	+ 0.07 %
100	5529	589	+ 0.09 %

The number of PI-cells have in impact mainly on the magnitude of the impedance and very little about the resonance frequency of the network. The choice of a cable model with 1 or 8 cell represents a difference of 16% on the value of the magnitude of the impedance.

To improve the choice of the number of cells needed for modeling this network, we note the impedances at different

frequency (Figure 9) depending on the number of cells.

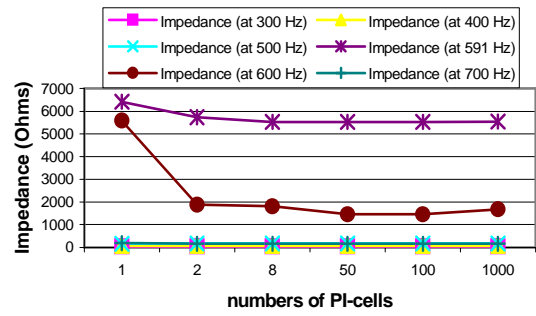


Fig. 9: Influence of the number of pi cells on the value of the impedance of the upstream network for different harmonic frequencies, up to 700 Hz.

Indeed, a single cell is not enough to model correctly the cable at high frequencies because its impedance doesn't vary linearly with the length and the frequency involved. In fact, the simulations performed with the EMTP-RV[5] program showed that the magnitude of the impedance reaches a constant value when eight cells are involved, which reinforces the need for a 8-cell modeling for the optimal modeling of the cable in that case.

This modeling has been adopted for the comparison between simulations and measurements made on the wind-farm site.

#### Zero sequence :

In that case, the injection is performed by applying the same voltage on the different phases at one end, and then connecting the other end of the cable directly to ground (zero sequence), as described below:

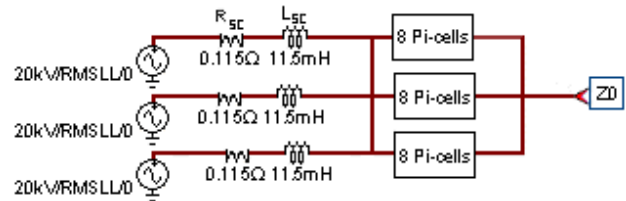


Fig. 10. Determination of the zero sequence impedance of the network.

TABLE III  
INFLUENCE OF THE NUMBER OF PI-CELLS ON THE IMPEDANCE OF THE NETWORK (ZERO SEQUENCE)

Number of Pi-cells	Impedance ( $\Omega$ )	Resonant frequency (Hz)	Discrepancies (with 8 Pi cells as the reference)
1	2168	597	+ 18 %
2	1912	593	+ 5 %
4	1856	593	+ 1.5 %
8	1830	591	0 %
16	1829	591	-0.06 %
50	1830	591	0 %
100	1840	592	+ 0.6 %

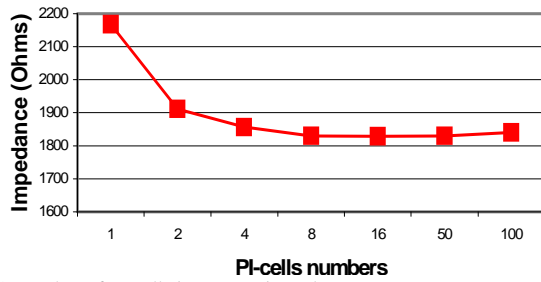


Fig. 11 Number of PI-cells impact on impedance.

As for the direct sequence, it confirms that 8 PI-cells lead to an appropriate modelling of the network .

### III. DETERMINATION OF THE FREQUENCY OF THE UPSTREAM NETWORK.

It is possible to deduce the frequency of the upstream network from the overvoltage appearing at the transformer entrance when energizing the MV cable, no loaded or connected to a transformer, as this frequency is present in the frequency response of this overvoltage.

The Department MIRE of the R&D, involved in the measurements on site, has performed the following  $V(t)/I(t)$  calculation at the entrance of the transformer, as shown in figure 12 below:

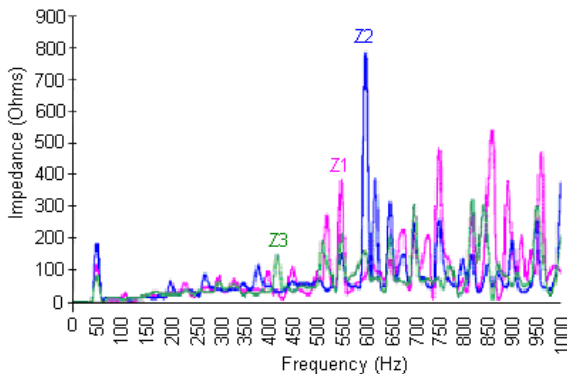


Fig. 12. Direct impedance versus frequency of the upstream 20 kV network.

It shows a frequency equal to 600 Hz, confirming the electrical characteristics of the upstream network, as previously mentioned.

The simulations performed in the variation range of the real short circuit values [108MVA-131MVA] showed that the resonance frequency of the network may vary between 590Hz and 640Hz.

Although this short circuit power was not explicitly given by the Distribution operator during the tests, it has been possible to determine a precise value of 110 MVA for the short circuit power at the secondary 20 kV side of the autotransformer, corresponding to the resonant frequency of 600 Hz; a voltage spectrum analysis has been performed on the overvoltage calculated at the entrance of the transformer, as shown in figure 13 below,

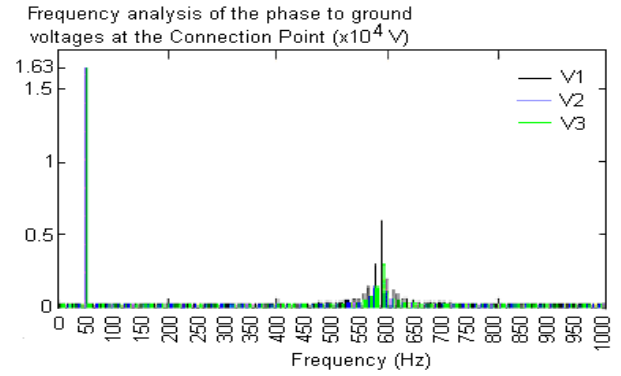


Fig. 13. Direct impedance versus frequency of the upstream 20 kV network.

### IV. COMPARISON BETWEEN SIMULATIONS AND ON SITE TESTS FOR THE ENERGIZATION OF ONE TRANSFORMER

#### A. Description of the network

The network is described by the following one line diagram, on figure 14 below:

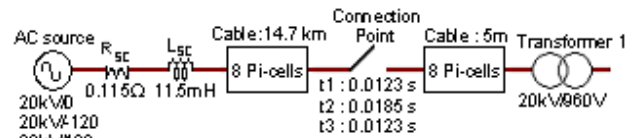


Fig. 14. Representation of the network when energizing one step-up transformer.

The MV cable is represented by 8 PI-cells, as previously mentioned in II, as we kept the same modelling, which could also be modelled by one pi cell, with no difference on the results.

All the simulations (inrush currents, voltage dips, overvoltages) have been performed at the CP, where the voltage divider was connected; in fact, the Connection Point is located at the interface of both networks, between the step-up transformers and the MV cable.

#### B. Determination of the initial conditions for the simulations

The initial conditions involved when energizing the step-up 2.05 MVA transformer are:

- The closing instants of the circuit breaker poles,
- The residual fluxes values circulating in the core of the target transformer before its energization (see table 4)

The closing instants are determined from the on site tests, from the times when the currents begin to rise through the circuit-breaker poles, which are respectively t1, t2 and t3 for phases A, B and C.

The residual fluxes are determined from the assumption that the maximum residual flux value of 0.8 p.u. (where 1 p.u. is equal to the nominal flux  $\phi_n$ , having a value of 2.5 Wb) is reached on one of the three phases, at the current zero crossing on the hysteretic curve, when opening the circuit-breaker before its energization.

For transformer 1 this value will remain stable, as there is no capacitive element connected directly to the transformer, which could lead, by forming an oscillatory circuit with the transformer inductance, to the damping of this residual flux; furthermore, the sum of the fluxes in the three limbs are equal to zero.

TABLE IV  
INITIAL CONDITIONS FOR THE SIMULATIONS IN THE CASE OF ONE TRANSFORMER ENERGIZATION

	Phase 1	Phase 2	Phase 3
Closing instants of the CB (in s)	0.0123	0.0185	0.0123
Residual fluxes in the transformer limbs (in p.u.)	0.8	-0.4	-0.4

### C. Determination of the inrush currents

Simulations have been made with these initial conditions, leading to the inrush currents of figure 15, which are very close to the ones measured on site, as shown in figure 16 below:

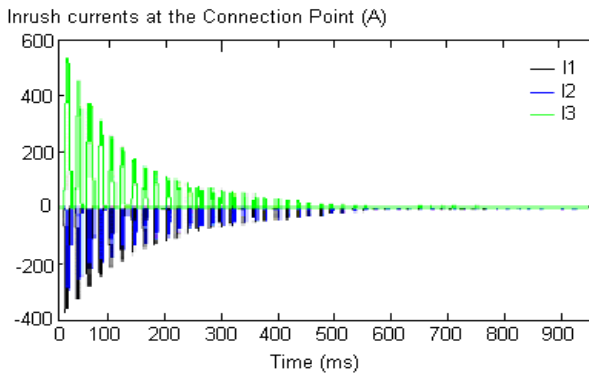


Fig. 15. Simulated inrush currents at the CP.

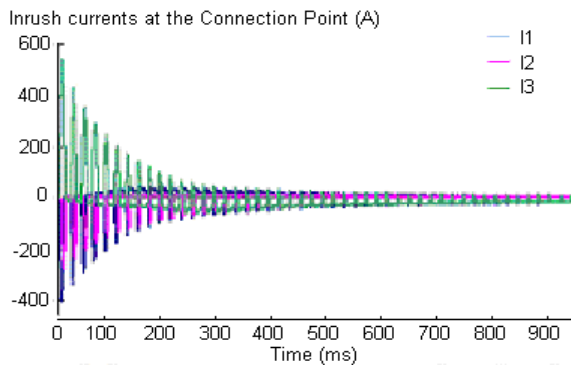


Fig. 16. Measured inrush currents at the CP.

The waveshapes from Figure 15 and Figure 16 show that the simulated waveforms are very close to those measured on site with similar amplitude values (see Table 2 below).

TABLE V  
COMPARISON BETWEEN SIMULATIONS AND MEASUREMENTS FOR INRUSH CURRENTS

	Simulation	Measurements	Discrepancies
Current I1	-397 A	-405 A	2 %
Current I2	-295 A	-285 A	3 %
Current I3	511 A	539 A	5 %

This confirms the fact that there are residual fluxes flowing in the transformer limbs after the opening of the circuit-breaker. Figures 17 and 18 show the frequency response of the inrush currents, simulated and measured respectively:

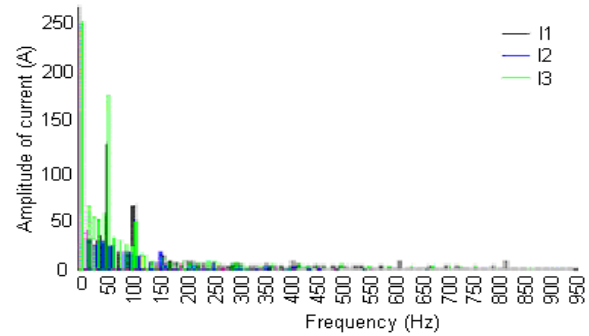


Fig. 17. Frequency response of the currents obtained from the simulations.

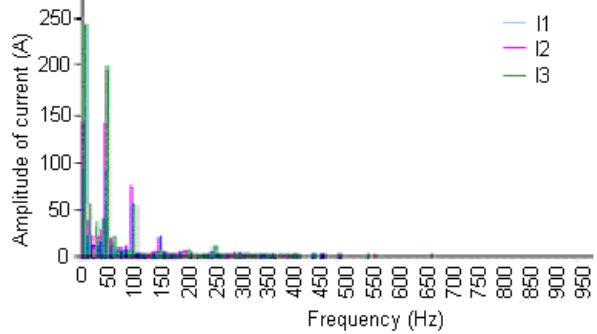


Fig. 18. Frequency response of the inrush currents measured on site.

The spectral analysis confirms the fact that inter-harmonics between two harmonics exist, and consequently the highly non linear magnetic behavior of those transformers. This can be explained by the fact that the value of the air-core reactance (given in p.u.) is low, due to the small size of the transformer and the low losses characteristics of the laminations of the iron core. The values obtained by simulations and measurements are given by the table 6 below:

TABLE VI  
COMPARISON BETWEEN SIMULATIONS AND MEASUREMENTS FOR INRUSH CURRENTS AMPLITUDES

	Simulation	Measurements	Discrepancies
Amplitude at 0 Hz	253 A	245 A	4%
Amplitude at 50 Hz	189 A	200 A	6%
Amplitude at 100 Hz	70 A	75 A	7%

#### D. Determination of the overvoltages at the transformer entrance

During the energization, harmonics generated by the transformer are injected through the upstream network, which may generate voltage-dips at the CP point and also overvoltages at the entrance of the transformer.

The overvoltages in that case are quite low, as shown in both simulations and measurements, and described below by figures 19,20 and 21 respectively:

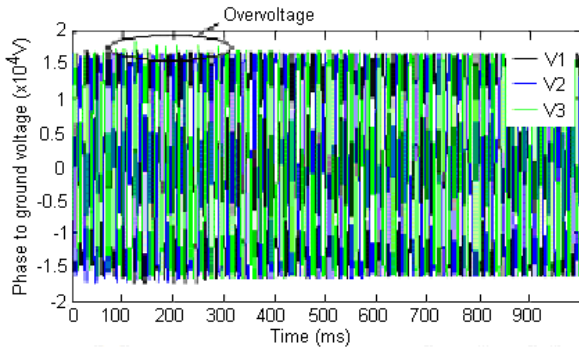


Fig. 19. Simulated overvoltages during a no load energization at the entrance of the transformer.

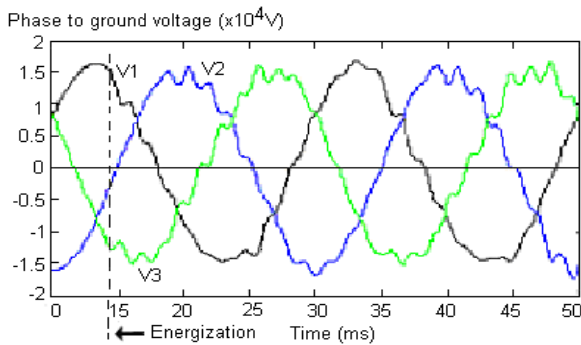


Fig. 20. Simulated overvoltages at the Connection Point during 2 periods.

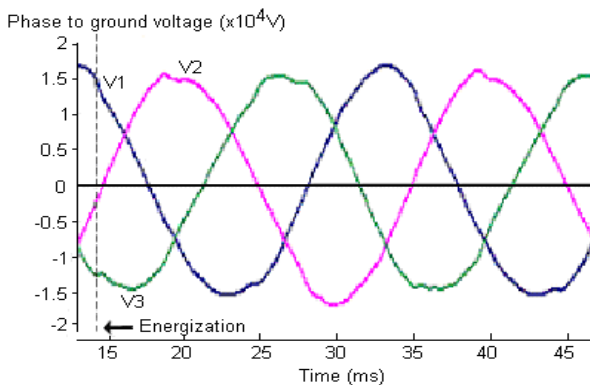


Fig. 21. Overvoltages measured at the Connection Point during 2 periods.

The overvoltage waveshapes are slightly more oscillatory in the simulations compared to the measurements on site; this may come from the modeling of the losses and especially the magnetic losses in the transformer, represented in that case by a single non linear core in parallel with a resistance; however, an hysteretic modeling of the saturation curve of the transformer gives similar results in that case.

It may also come from the fact that the measurements have been performed with an active filter located at the CP; another origin may come from the fact that the upstream network is only represented by its short-circuit power, this hypothesis being however acceptable as the short-circuit power is high, due to its connection to the Distribution Network.

The results obtained validate the modeling proposed, as well as the assumptions considered on the initial conditions and also the value of short circuit power derived from the on site tests.

#### V. CONCLUSION

This paper describes the phenomena involved in a 10 MW wind-farm, located in the North of France, when energizing the 2.05 MVA 20kV/960V step-up transformers.

A detailed modeling of the network and equipment under the phenomena involved has been described

A comparison between simulations and on site tests is presented in the case of the energization of one transformer, secondly in the case where three others transformers are previously energized, showing a good agreement between simulations and measurements.

#### VI. ACKNOWLEDGMENT

The authors would like to thank S. Denettière, X. Legrand of the Departement THEMIS and T. Kermaol of the Meotec Company, involved respectively in the EMTP-RV developments and the modeling of wind-farms.

#### VII. REFERENCES

##### Papers from Conference Proceedings (Published):

- [1] T. Ackermann, E. Centeno Lopez, L. Söder, "Grid Connection Rules for Wind Farms in Spain, Germany, Portugal, UK, and Sweden", 7th International Workshop on Large-Scale Integration of Wind Power into Power Systems, Madrid, May 2008.
- [2] A. Narang, R.H. Brierley, "Topology based magnetic model for steady-state and transient studies for three-phase core type transformer", IEEE Transactions on Power Systems, Vol. 9, No. 3, August 1994.
- [3] W.L.A. Neves, H.W. Dommel, "Saturation curves of delta-connected transformers from measurements", IEEE, No. 94 SM 459-8 PWRD, July 1994.
- [4] R. King, N. Jenkins "Switching transient in large offshore windfarms" 7th International Workshop on Large-Scale Integration of Wind Power into Power Systems, Madrid, May 2008.

##### Periodicals:

- [5] J. Mahseredjian, S. Denettière, L. Dubé, B. Khodabakhchian, L. Gérin-Lajoie, "On a new approach for the simulation of transient in power systems" Electrical Power System Research, Volume 77, Issue 11, Sept.2007 pp.1514-1520.
- [6] P. Johannet "A fine modelling of cables in harmonic or transient cases by inverse Laplace transform." JICABLE 91 - Report B.6.2.
- [7] E.Dorison, J. Lepers, B.Riot "Optimization criteria of the transmission capacity of HV and VHV cables". JICABLE 91 - Report B.7.4